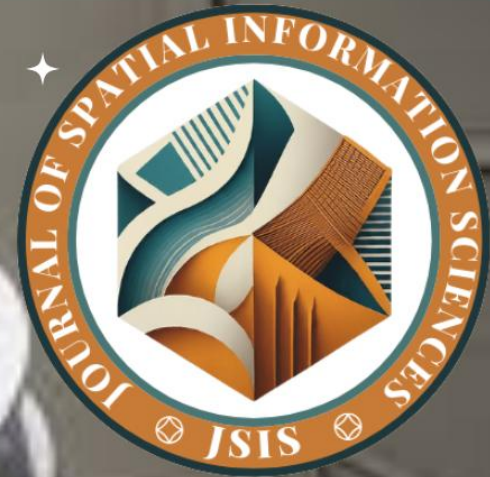


Journal of
Spatial
Information
Sciences

...JSIS



**A COMPUTATIONAL TOOL FOR LOCAL
GRAVIMETRIC GEOID DETERMINATION
USING LEAST SQUARES COLLOCATION**

**Tukka, A. Apollos, Tata, Herbert
Idowu, O. Timothy**





A COMPUTATIONAL TOOL FOR LOCAL GRAVIMETRIC GEOID DETERMINATION USING LEAST SQUARES COLLOCATION

¹TUKKA, A. Apollos; ²TATA, Herbert; ³IDOWU, O. Timothy

^{1,2,3}Dept. of Surveying and Geoinformatics, School of Environmental Technology, Federal University of Technology Akure (FUTA), Ondo State, Nigeria.

Corresponding author: ¹aatukka@futa.edu.ng

DOI: <https://doi.org/10.5281/zenodo.14961951>

Abstract

This study presents a computational tool (TUIDOTA), for determining local gravimetric geoids using Least Squares Collocation (LSC) techniques, essential for geodetic applications. The geoid provides a reference surface for determining the height of the earth's surface. The study focuses on evaluating the potential of the tool within Akure South Local Government Area in Ondo State of Nigeria, representing mountainous terrains. High-quality terrestrial gravity data, geopotential, and digital elevation models were used. The developed tool facilitates the selection between SLSC and NSLSC, making computations and output visualization straightforward. Results included geoidal undulations, processing time, and geoidal maps. For the pairwise comparisons of geoidal undulation, this indicates that the difference between (SLSC) and (NSLSC) techniques is not statistically significant, having a mean difference of -0.020m ($SE = 0.036\text{m}$, $p = 0.567$) and a 95% confidence interval of $[-0.090\text{m}, 0.049\text{m}]$. This result remains consistent under a 99.9% confidence interval, which spans $[-0.137\text{m}, 0.097\text{m}]$. However, for processing time, there exists a highly significant difference between the two techniques. The SLSC technique was 30.459 seconds faster than the NSLSC ($SE = 0.000$, $p < 0.001$), with a confidence interval of $[-30.459, -30.459]$ in terms of both 95% and 99.9% levels. Also, using the GGM dataset for both approaches, the standard deviations for both approaches yielded 1.538476m and 1.538454m respectively. Furthermore, using the DEM dataset for both approaches, the standard deviations for both approaches yielded 0.943200m and 0.943198m respectively. TUIDOTA proved to be effective, accurate, economical, and user-friendly, and it is hereby recommended for local geoid determination.

Keywords: Computational tool, Gravimetric geoid, Least Squares Collocation, Molodensky model, TUIDOTA

1.0 INTRODUCTION

According to [3] the geoid, which closely approximates mean sea level, serves as a reference surface for determining orthometric heights. The geoid in geodetic studies can be determined at a local, regional, or global scale as a Potential function [14] The determination of such a potential function is related to the field of Applied Mathematical Physics and is normally referred to as the "Geodetic Boundary-Value Problem" in Physical Geodesy. The need for the geoid in physical geodesy is to serve as a reference surface or benchmark for orthometric



heightening which is usually determined by spirit leveling [27]. This is of great importance not only for scientific fields like: geodesy, geodynamics, geophysics, and geology but also in various surveying practices. According to [24], "The geoid represents an equipotential surface of the Earth's gravity field that best fits the global mean sea level in the Least square sense." Meanwhile, today, with the immense progress made in the Global Navigation Satellite System (GNSS), there exists efficiency in determining horizontal and vertical positions on the Earth's surface by providing the geodetic community and also users of geodetic products an opportunity to establish height of any point above the reference ellipsoid everywhere and anywhere on the Earth's surface [33].

However, in spirit levelling, the error increases with the distance from the levelling network and requires a lot of effort, man-hour time and resources [33]. In the intervening period, the reference ellipsoid represent a mathematical surface that approximates the terrestrial surface of the Earth, but does not coincide with the precise figure or to the geoid surface [14]. Accurate determination of the geoid height at any observation station is possible if a stipulated standard and high level of consistency is sustained. Furthermore, if the measurement of geoid height (N) above an ellipsoid and along the ellipsoidal Normal is possible at a certain position, then any ellipsoid height (h) measured on the Earth's surface above such reference ellipsoid could be converted to Orthometric height (H) for any point (K) on the Earth's surface [37]. This measured height along the plumbline can replace the need for spirit levelling, by applying a simple mathematical expression yielded by Equation (1) as:

$$H = h - N \pm \sum Ortho \quad (1)$$

The widely used methods for determining the geoid can be grouped under the GPS/levelling technique, moreover known as the geometric approach. There are other methods as well, such as the combined geometric/gravimetric method, satellite method, geodetic method, and gravimetric method to mention but a few. The development of a computational tool for the determination of local gravimetric geoid, using gravimetric techniques based on the application of the least squares collocation approach integrated with the Molodensky algorithm is the focus of this study. Through the use of appropriate covariance functions that account for spatial dependencies in the observed data a-sets, the LSC technique serves as a bridge between the physical and statistical perspectives on various gravity field parameters ([19]; [21]; [26]; [27]; [29]; [32])

A study conducted by [7] reveals that the geoid can be determined using the Stationary Least Square Collocation (SLSC) and Nonstationary Least Square Collocation (NSLSC) techniques. The notion of SLSC is frequently utilized in classical geodesy. The notion is founded on the concepts that the observed dataset's mean remains constant throughout the research region and that the covariance function utilized is isotropic, meaning it acquires a uniform shape in every direction. Additionally, it is dependent only on the separation distance between the observations ([19]; [26]; [27]; [28]; [32]; [34]; [40]). Although the geoid determination process is convenient due to these assumptions, it is not always realistic for all regions [32]. The NSLSC approach was discovered through further review, and is thought to be a superior substitute method currently employed in the spatial sciences, including geodetic research [7]. The methodology relies on the idea that the designed covariance function is anisotropic, meaning it varies with direction and that the mean of a dataset is not always constant. Consequently, in order to determine the local gravimetric geoid, this alternative LSC approach must be domesticated because it displays non-stationarity in the covariance function structure [6]; [22]; [23]; [25]

1.1 Computational Tool for Gravimetric Geoid Estimation Based on LSC Technique



www.journals.unizik.edu.ng/jsis

According to ([6];[11]) the introduction of the GRAVSOFTE package of FORTRAN77 programs by [38] was a turning point in application and adoption. GRAVSOFTE has been updated regularly since 1994. It includes different program modules for the determination of empirical covariance function (EMPCOV), its analytical modeling (COVFIT), geoid determination using LSC, the computation of an approximation to the anomalous potential of the Earth using Stepwise (GEOCOL), the evaluation of Spherical Harmonic series, Datum Transformations and Planar. The computational tool has been utilized around the world for diverse applications of LSC in geodesy; and compared with other estimation techniques like the Fast Fourier transform (FFT) and Numerical integration ([4]; [8]; [9]; [12];[15]; [18]; [42]) and proved the efficiency of the LSC technique in geoscience for estimation and prediction in local and global scales. However, when using GRAVSOFTE, computations therein are performed in batch mode, making it non-interactive, and the covariance function representation is implemented operating only an isotropic kernel, fitted to the empirical covariance function [20]. This fundamental structure of the covariance model (isotropic) causes difficulties when the technique is applied in an area with a strong non-isotropic gravity field, such as a mountain chain or a fault [6].

Meanwhile, aside from the fact that this existing computational tool was based on LSC [38] and primarily designed for global or broad regional scale geoid modelling; most at times it is not universally coherent posing a challenge for non-specialist users to operate and use a covariance function that suffers the problem of terrain smoothing [6]. In addition, these existing software packages mostly require a comprehensive geoid model to understand and utilize them properly [10]. For instance, users are required to generate numerous input files and manipulate multiple batch scripts to obtain the eventual solution of the geoid model, which represent processes that repeatedly extract a considerable amount of time([3]; [41]; [42]). Recently, a compact and user-friendly software package called “CSHSOFTE” was developed and presented for scholars in the field of geoid modeling [3]. Here, a fractionated programming strategy was adopted to build its individual components striving for unerring accuracy and computational efficiency for geoid heights. However, the “CSHSOFTE” was designed to evaluate the Classical Stokes-Helmert algorithm. In the same way [1] developed a practical software package for computing the gravimetric geoid by the least squares modification of Hotine’s formula. [2] still avail another software package for computing a regional gravimetric geoid model implementing the KTH method. In the same way, among other computational tools that are not based on LSC technique or Molodensky algorithm, [36] developed a computational tool for the determination of local geoid using gravimetric and GPS/Levelling based on Stokes function and corrector surface approach. Least Squares Collocation (LSC) provides a robust statistical framework for geoid determination, modeling spatial dependencies in gravity field parameters (Moritz, 1980). Traditional computational tools like GRAVSOFTE [38] have been widely adopted but remain batch-mode dependent, require extensive training, and often assume isotropic covariance functions, which may not hold in complex terrains [7] More recent tools, such as CSHSOFT, focus on classical Stokes-Helmert methods but do not integrate LSC techniques [3].

With all these novel studies, the literature reviewed thus far suggests that, consideration was not given to the development of a computational tool based on the LSC technique integrated with the Molodensky algorithm[5]. It is therefore necessary and justifiable to develop a computational tool that is user-friendly for the determination of the local gravimetric geoid using the least squares (LSC) technique based on the Molodensky method [30].



Hence, In contrast, the TUIDOTA is specifically designed to provide an interactive, user-friendly interface for local geoid determination using both SLSC and NSLSC methods. This study aims to evaluate its efficiency and accuracy in a real-world setting.

2.0. STUDY AREA

Due to the availability of data and the need to compute differences in the properties of the gravitational field across mountainous locations, the study focuses on Akure South LGA in Ondo State located within the rainforest belt of Nigeria and lies between latitude $07^{\circ} 14' 50'' \text{N}$ and $07^{\circ} 18' 30'' \text{N}$ and longitudes $05^{\circ} 08' 40'' \text{E}$ and $05^{\circ} 12' 05'' \text{E}$ ([16];[17]). Figure 1 shows the area used to evaluate the computational tool efficacy using the SLSC and NSLSC technique based on the Molodensky algorithm, within the framework of the Remove-Compute-Restore (R-C-R) technique in determining the local gravimetric geoid within the study area. This study primarily relied on secondary datasets, within the study area these includes: Geopotential Models from various satellite missions (EGM2008, SGG-UGM-2, and XGM2019e_2156) and terrestrial gravity data from [36] which represent mountainous terrains. The Global Geopotential Model and Digital Elevation Models were obtained from the International Centre for Global Earth Model (ICGEM)[15] and the United States Geological Survey's Earth Explorer, respectively[39]. The reliability and accuracy of the input datasets were verified from these sources, along with validation datasets consisting of GPS/levelling data and Gravimetric geoid models.

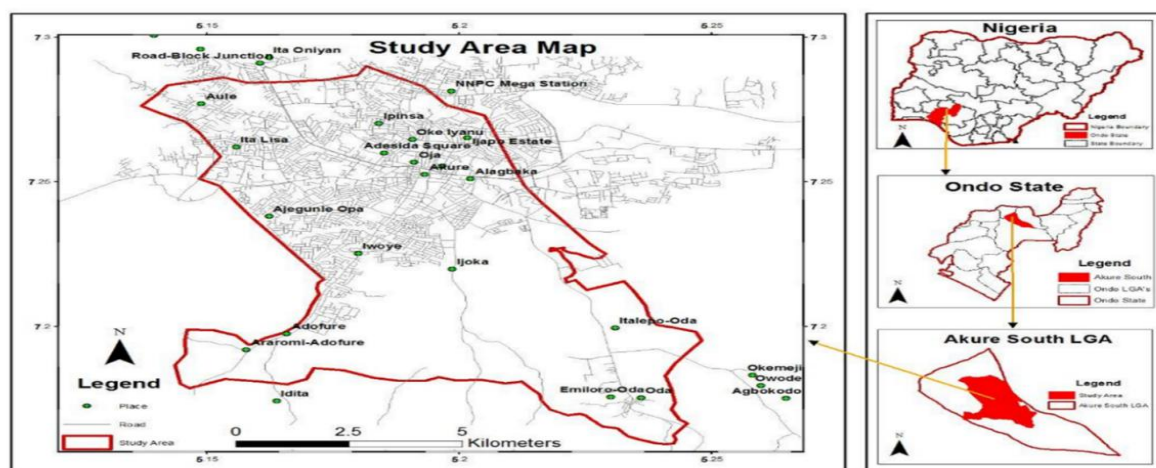


Figure 1: Ondo State in Nigeria. Source: [36]

3.0 MATERIALS AND METHODS

The research methodology includes data collection, quality assessment, presentation, and processing to achieve the desired results as shown in Figure 2.

3.1 Development of computational tools for data processing

In the R programming environment, all the necessary parameters for developing the computational tool for local gravimetric geoid determination were input, as illustrated in Figure 2. This process involved adopting and modifying the Convo-SPAT package [31], where the



Molodensky method for geoid determination using Least Squares Collocation (LSC) was coded and applied for geodetic applications. Sample of R-Code for the

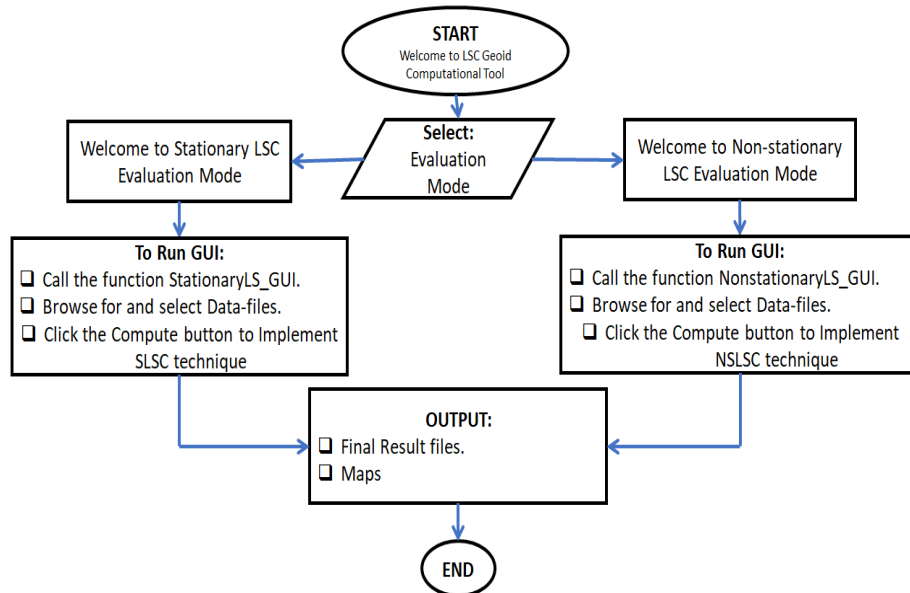


Figure 2: Flowchart of Developed Computational Tool

```

library(convoSPAT)
library(gstat)
library(sp)
library(sf)
library(viridis)
library(stringr)
library(metR)
maymac = fluidPage(
  useShinyjs(),
  sidebarLayout(
    sidebarPanel(
      radioGroupButtons("fitting", label = "Select Fitting Type", choiceName=c("Stationary",
"Non-Stationary"), choiceValues=c("aniso", "NS"), selected = "NS"),
      selectInput("cov.model", "Covariance Model",
        choices = c("Gaussian" = "gaussian", "Exponential" = "exponential", "Matern" =
"matern"))
      selectInput("gloAno", "Global Anomaly Model",
        choices = c("EGM" = "EGM", "SGG" = "SGG", "XGM" = "XGM")),
      selectInput("Elev_srtm", "Digital Elevation Model",
        choices = c("ALOS" = "ALOS", "ASTER" = "ASTER", "TANDEM" =
"TANDEM")),
      fileInput("obs_file", "Choose CSV File - Observation File"),
      h6("Prediction Data") checkboxInput("pred_check", "Same As Observed").

```

Figure 3 : Snippet of part of initialization code for the Computational tool (TUIDOTA)



3.2 Data Processing

The computational process was adopted for the study in three phases as shown in Figure 4. Phase one (1) involves preliminary processing which consists of steps 1 to step 5; while phase (2) involves the fitting of alternative spatial (Stationary and Non-Stationary) models which consists of steps 6 and step 7. And lastly, phase 3 consists of steps 8 and step 9.

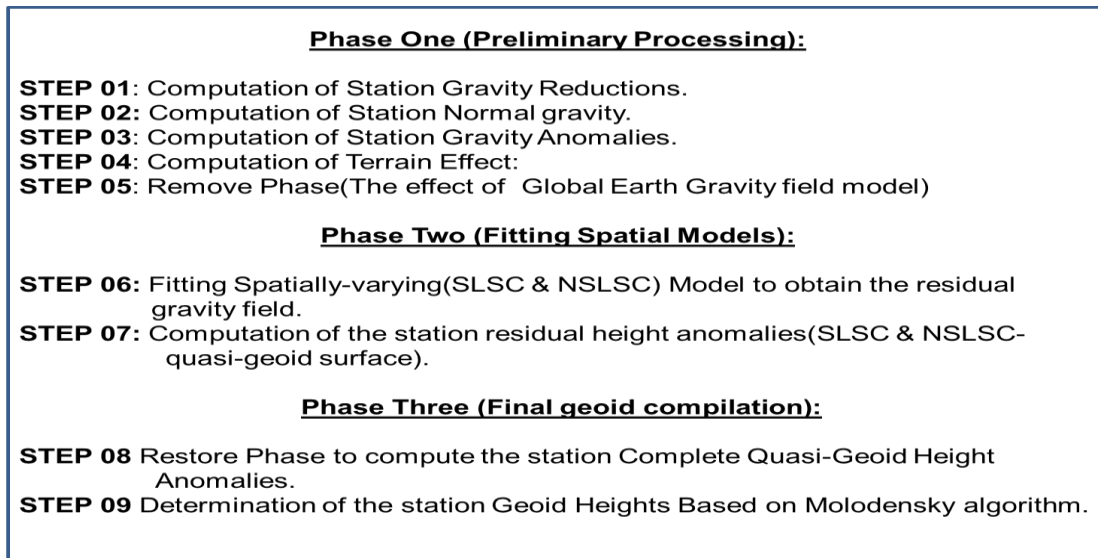


Figure 4: Snippet of the Three phase computational process strategies.

3.3 Research Hypothesis

Two hypotheses were formulated for this study:

1). Null Hypothesis (H_{0_1}): There is no significant differences in the Mean computed between the results obtained from SLSC and NSLSC techniques in the estimated local gravimetric geoid. These are mathematically expressed as:

$$H_{0_1}: \mu^{SLSC} = \mu^{NSLSC} \tag{2}$$

Alternative Hypothesis (H_{A_1}): There is. These are mathematically expressed as:

$$H_{A_1}: \mu^{SLSC} \neq \mu^{NSLSC} \tag{3}$$

where: SLSC = Stationary and NSLSC = Nonstationary covariance approaches.

2). Null Hypothesis (H_{0_2}): There is no significant difference between the Mean of computed Best-fit (Optimum) model values obtained from hypothesis test (1) above and those obtained from existing Gravimetric, GPS/Leveling geoidal undulations and Orthometric heights of the stations. These are mathematically expressed as:

$$H_{0_2_i}: \mu^{BEST-fit} = \mu_{Gravimetric}^{Existing} \tag{4a}$$

$$H_{0_2_j}: \mu^{BEST-fit} = \mu_{GPS/Leveling}^{Existing} \tag{5a}$$



$$H_{0_{2k}} : \mu^{\text{BEST-fit}} = \mu_{\text{Orthometrics}}^{\text{Existing}} \tag{6a}$$

Alternative Hypothesis (H_{A4}): There is. These are mathematically expressed as:

$$H_{A_{2i}} : \mu^{\text{BEST-fit}} \neq \mu_{\text{Gravimetric}}^{\text{Existing}} \tag{4b}$$

$$H_{A_{2j}} : \mu^{\text{BEST-fit}} \neq \mu_{\text{GPS/Leveling}}^{\text{Existing}} \tag{5b}$$

$$H_{A_{2k}} : \mu^{\text{BEST-fit}} \neq \mu_{\text{Orthometric Heights}}^{\text{Existing}} \tag{6b}$$

3.4 Statistical analysis

In this study, the test of the null hypothesis 1 was implemented using SPSS (23) version’s sub-routine, predefined for MANOVA via the General Linear Model (GLM) at both 95% and 99.9% confidence interval for SLSC and NSLSC respectively. For hypothesis two, the study implemented the Paired Samples Statistics, Correlation, and T-Test to compare the means of two or more related groups and determine if a significant difference existed between paired observations. This analysis was also conducted at 95% and 99.9% confidence intervals.

4.0 RESULTS AND DISCUSSION

4.1 The Computational Tool “TUIDOTA”

Figure 5 displays a screenshot of the developed computational tool (TUIDOTA) graphic user interface (GUI), where the analysis scenario was set up using the Stationary fitting technique. This was activated with the Matérn covariance model, the SGG global anomaly model, and the TANDEM DEM, along with observational data from Akure.csv. The software generated a contour map of geoidal undulation, allowing for an efficient visualization of variations in geoidal heights across the study area. The tool provides options to select novel fitting techniques, covariance models, global anomaly models, and digital elevation models. The interface supports user-friendly interaction by enabling data uploads, geoidal data downloads in .csv format, displaying processing time (Total Runtime), and exporting contour maps. In summary, the visualization effectively highlights spatial variations in geoidal undulation and offers a platform for further analysis and model comparisons.

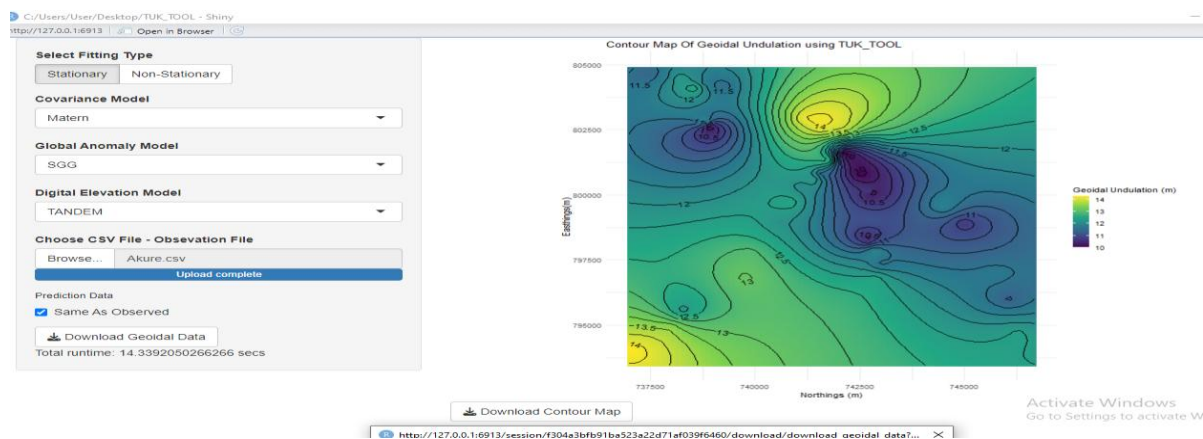


Figure 5: Screen short of the computational tool “TUIDOTA” graphic user interface (GUI).



4.1.1 The Computational Tool “TUIDOTA” outputted results

In this study, the datasets obtained were employed within the mathematical formulations previously outlined summarily in steps 1 to 9 of the Snippet in Figure 4. These were estimations based on the LSC-Molodensky methodology consisting of Compute-Remove-Restore approach. Table 1 presents the results from the most suitable model (Matern, SGG-GGM & ALOS-DEM), showing residual field values, residual height anomaly, quasi-geoid height anomaly, and geoidal height for different stations along with their coordinates and orthometric heights

Table 1: Results obtained from the most suitable model (Matern, SGG-GGM & ALOS-DEM)

S/N	Station	X(m)	Y(m)	Phase Two		Phase Three		Orthometric Height (m)
				Residual Field (m)	Residual Height Anomaly (m)	Quasi Height Anomaly (m)	Geoidal Height (m)	
1	GPSA72S	739272.08	804184.37	-16.4488	-0.3387	13.3614	13.3766	333.0933
2	GPSA73S	739057.83	804174.63	-16.4494	-0.3398	13.4385	13.4536	331.6928
3	GPSA75S	738721.93	804299.37	-16.4621	-0.3454	13.8235	13.8381	324.5498
4	GPSA76S	738465.8	804373.82	-16.4699	-0.3470	13.9205	13.9350	322.7309
5	GPSA77S	738143.72	804499.99	-16.4822	-0.3489	14.0331	14.0474	320.6035

Concurrently, the computational tool extracted the following statistics for the station geoidal undulation and processing time results. Tables 2a and 2b present the statistics of station geoidal undulation and processing time for SLSC and NSLSC techniques at 95% and 99.9% confidence intervals, showing the mean values, standard errors, and confidence bounds.

Table 2a: Statistics of station geoidal undulation and processing time at 95% C.I.)

Estimates					
Dependent Variable	LSC Techniques	Mean	Std. Error	95% Confidence Interval	
				Lower Bound	Upper Bound
Geoidal Undulation	SLSC	14.273 ^a	0.025	14.224	14.323
	NSLSC	14.294 ^a	0.025	14.244	14.343
Processing Time	SLSC	8.210 ^a	0.000	8.210	8.210
	NSLSC	38.669 ^a	0.000	38.669	38.669

Table 2b: Statistics of station geoidal undulation and processing time at 99.9%(C.I.)

Estimates				
Dependent Variable	LSC Techniques	Mean	Std. Error	99.9% Confidence Interval



				Lower Bound	Upper Bound
Geoidal Undulation	SLSC	14.273 ^a	0.025	14.190	14.356
	NLSLC	14.294 ^a	0.025	14.211	14.376
ProcessingTime (Seconds)	SLSC	8.210 ^a	0.000	8.210	8.210
	NLSLC	38.669 ^a	0.000	38.669	38.669

Figure 6 compares the estimated marginal means (EMM) of geoidal undulation for the Akure study area using SLSC and NSLSC techniques.

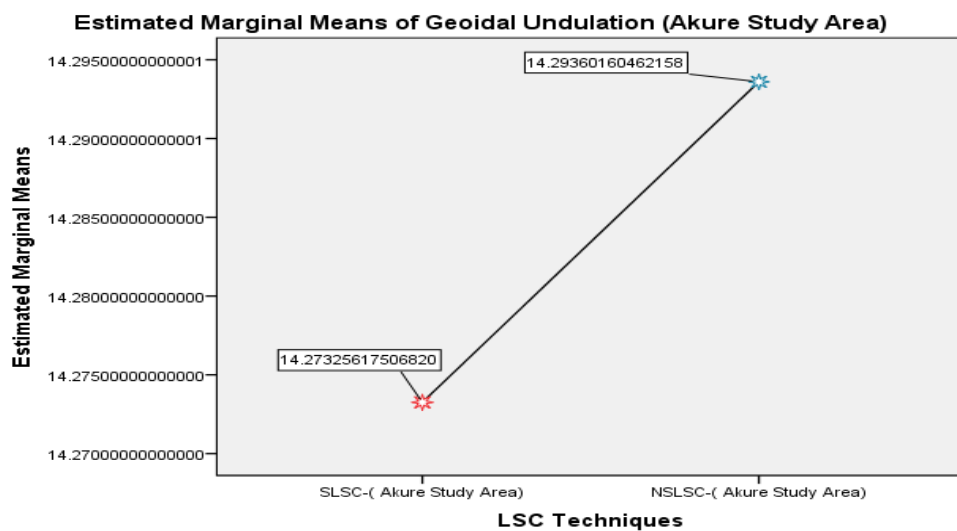


Figure 6: Comparison of EMM of Geoidal Undulation based on SLSC and NSLSC techniques.

Figure 7 compares the estimated marginal means of processing time for SLSC and NSLSC techniques using the TUIDOTA software.

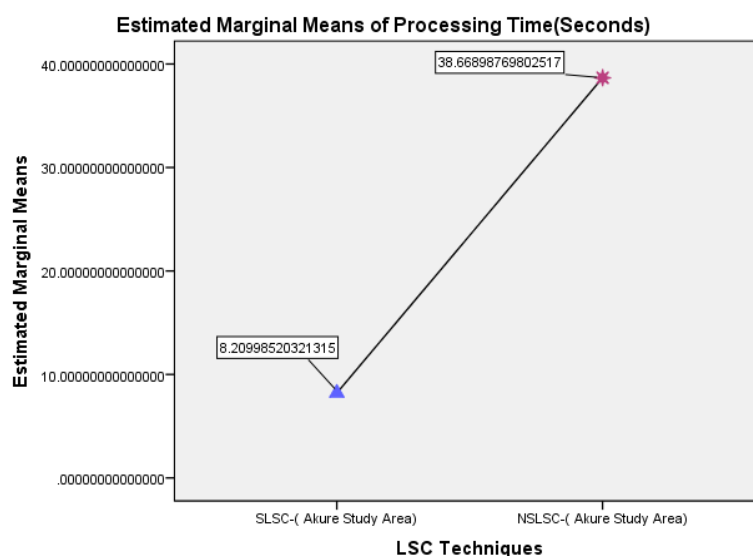




Figure 7: Comparison of software (TUIDOTA) processing time based on SLSC and NSLSC

Figure 8 compares the estimated marginal means of geoidal undulation in the Akure study area for different covariance models.

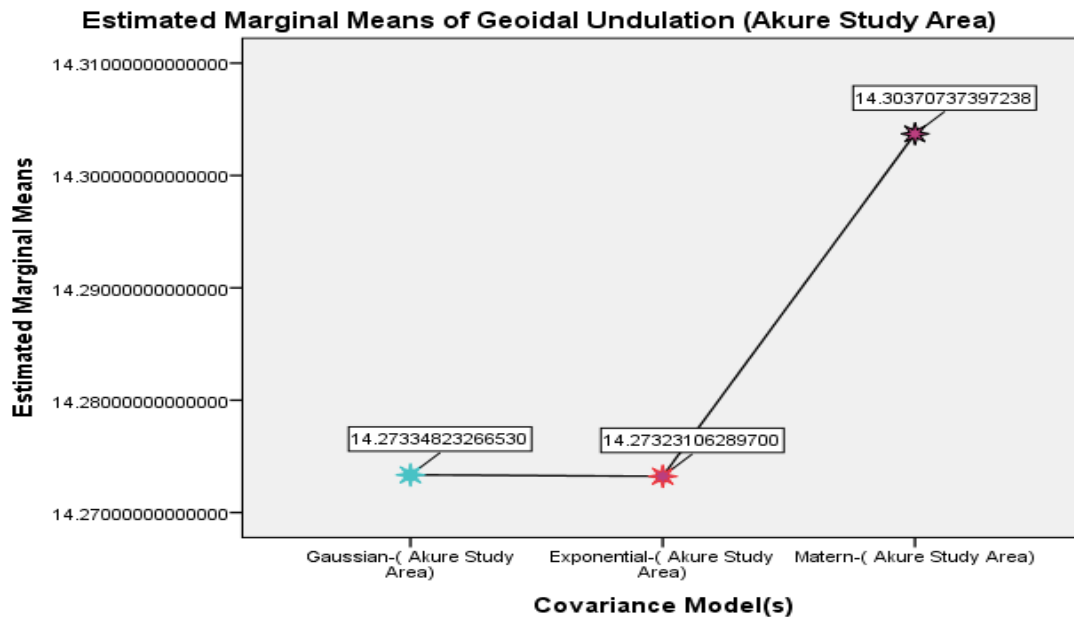


Figure 8: Comparison of Geoidal Undulation based on different covariance models

Figure 9 compares the estimated marginal means of processing time for the different covariance models, using the TUIDOTA software.

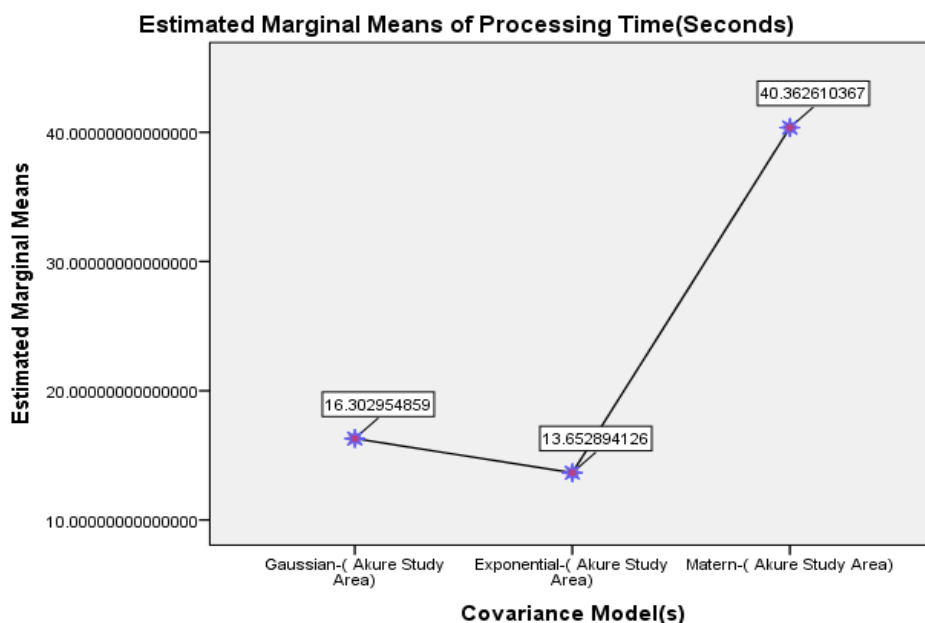


Figure 9: Processing time based on covariance models.



Figure 10, 11 and 12 presents the estimated marginal means of geoidal undulation for the Akure study area using the EGM2008, SGG-UM and XGM2019e-global geoid model respectively. It compares the results from different covariance models (Gaussian, Exponential, and Matern) for both SLSC and NSLSC techniques, showing variations in geoidal undulation values across methods.

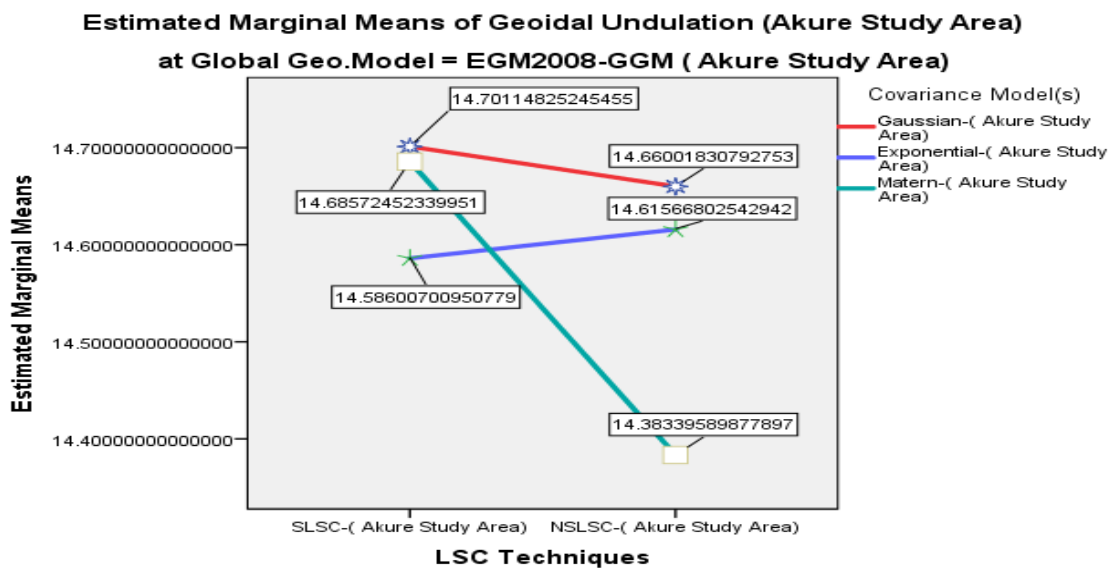


Figure 10: Comparison of geoidal undulation based on EGM2008-GGM model

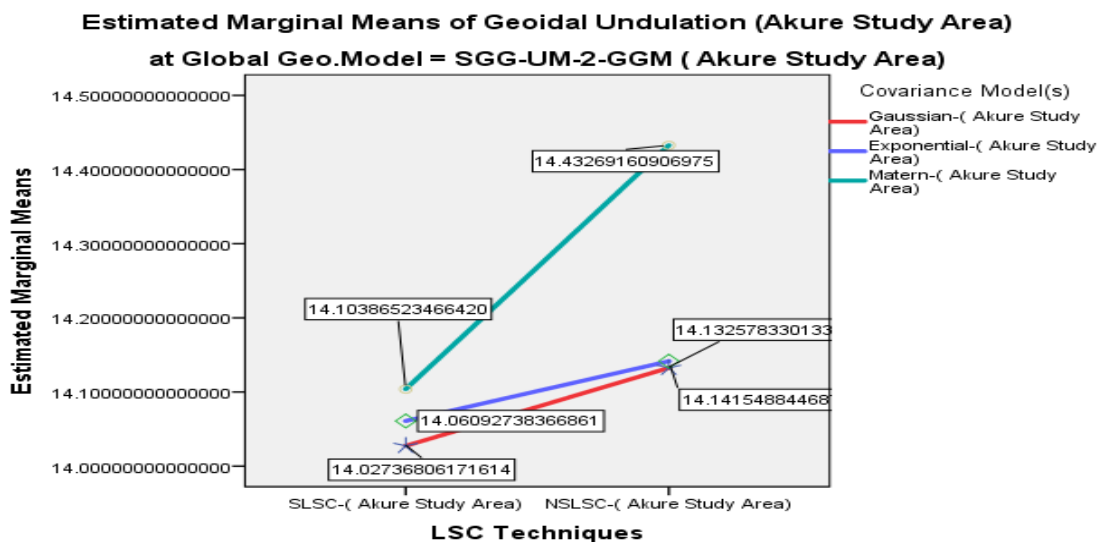


Figure 11: Comparison of geoidal undulation based on SGG-UM-GGM model

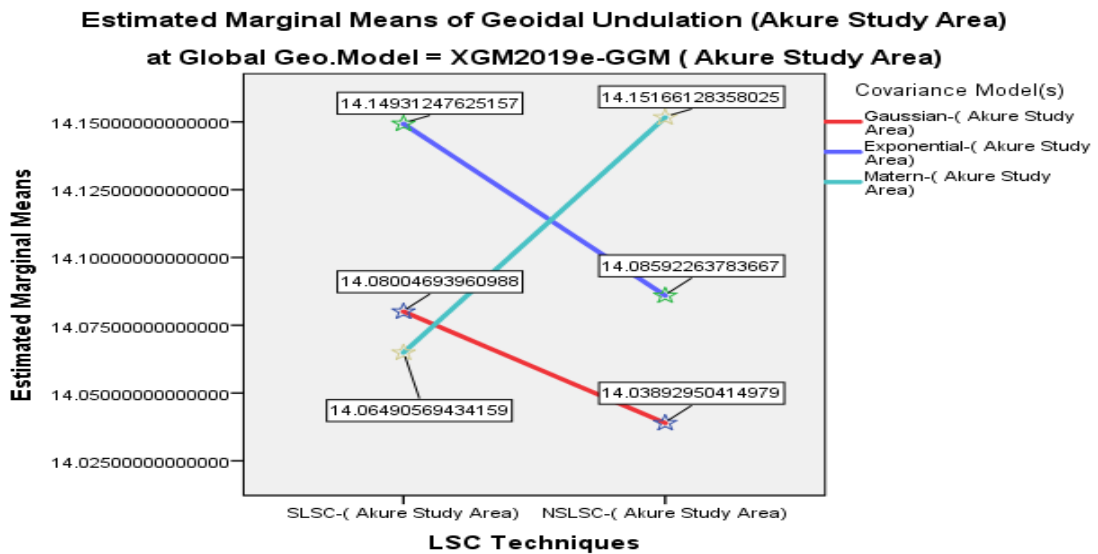


Figure 12: Comparison of geoidal undulation based on XGM2019e-GGM model

Figure 13, 14 and 15 presents the estimated marginal means of geoidal undulation for the Akure study area using the ALOS PALSAR, ASTER and TANDEM Digital Elevation Model (DEM) respectively. It compares the results from different covariance models (Gaussian, Exponential, and Matern) for both SLSC and NSLSC techniques, showing variations in geoidal undulation values across methods

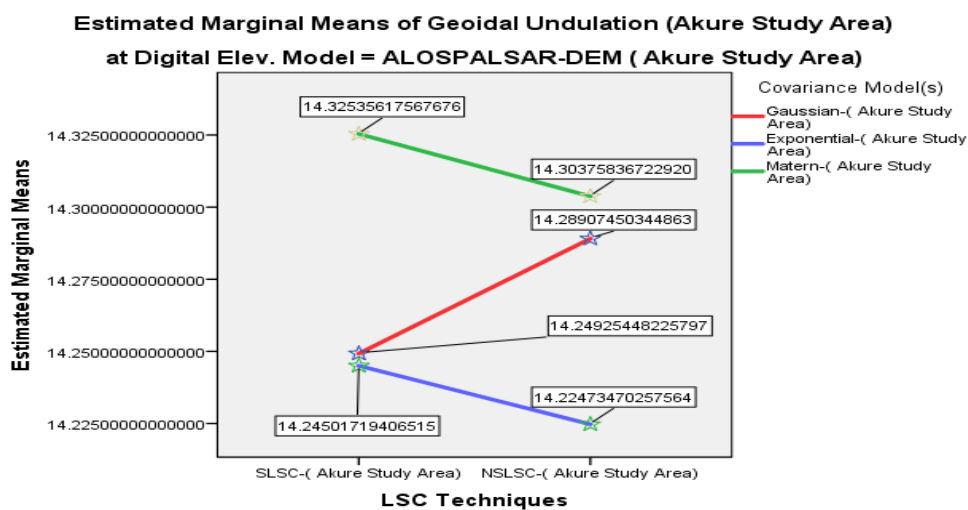


Figure 13: Comparison of geoidal undulation based on ALOS-PALSAR-DEM model

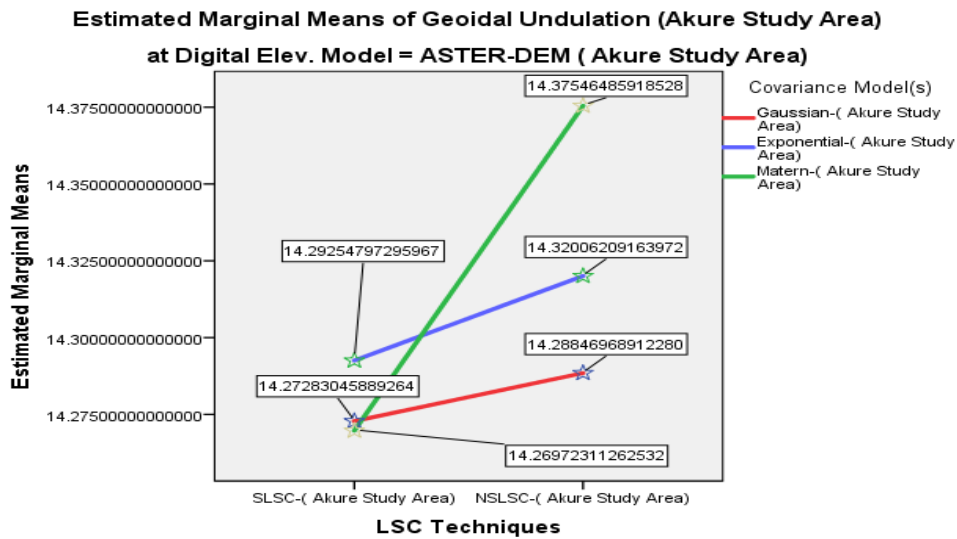


Figure 14: Comparison of geoidal undulation based on ASTER-DEM model

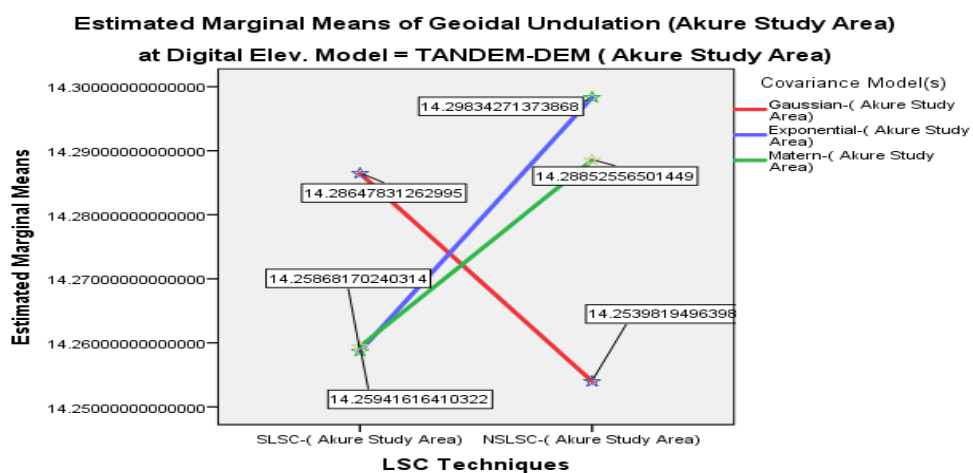


Figure 15: Comparison of geoidal undulation based on TANDEM-DEM model

Figure 16 compares the best-fitted geoidal undulation model with existing models (GRAV and GPS/LEVEL) within the Akure study area. The variations in geoidal undulation across different ground stations are shown, highlighting the differences between the computed and existing models.

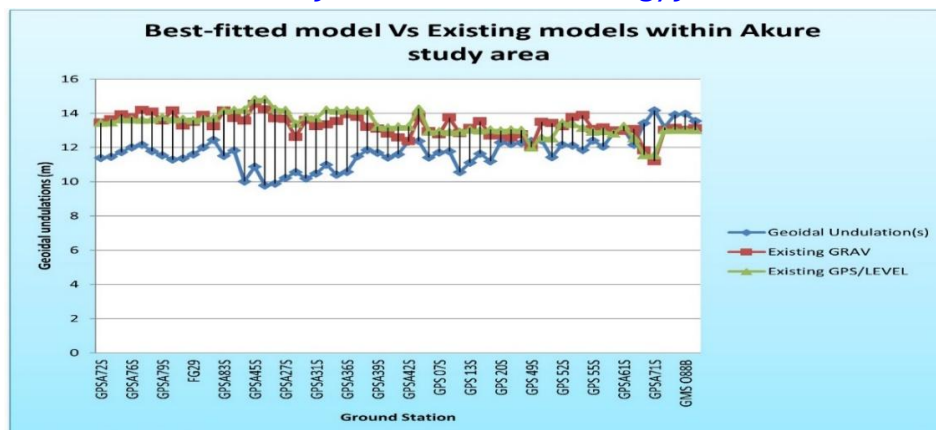


Figure 16: Best-Fitted Model (TUIDOTA) and Existing Models

4.1.2 Statistical Test results

Here, Pair-wise comparison results for SLSC and NSLSC outputted at 95% and 99.9% Confidence Interval from the package are summarized in Tables 3 and 4 respectively. While, results of Paired Samples Correlations and Paired samples T-test. were implemented using SPSS version 23 subroutine at 95% and 99.9% Confidence Interval (C.I.) in Tables 5, 6, and 7 for the study area.

Table 3 presents the mean differences in geoidal undulation and processing time between SLSC and NSLSC techniques for hypothesis testing at a 95% confidence level.

Table 3: Mean Differences needed for Hypothesis testing one (1) at 95% (C.I.)

Pairwise Comparisons							
Dependent Variable	(I) LSC Techniques	(J) LSC Techniques	Mean Difference (I-J)	Std. Error	Sig. ^b	95% Confidence Interval for Difference ^b	
						Lower Bound	Upper Bound
Geoidal Undulation	SLSC	NSLSC	-0.020	0.036	0.567	-0.090	0.049
	NSLSC	SLSC	0.020	0.036	0.567	-0.049	0.090
Processing Time (Seconds)	SLSC	NSLSC	-30.459*	0.000	0.000	-30.459	-30.459
	NSLSC	SLSC	30.459*	0.000	0.000	30.459	30.459

Based on estimated marginal means*. The outstanding difference is significant at the .05 level. b. Adjustment for multiple comparisons: Least Significant Difference (equivalent to no adjustment).

Table 4 presents the mean differences in geoidal undulation and processing time between SLSC and NSLSC techniques for hypothesis testing at a 99.9% confidence level.

Table 4: Mean Differences for Hypothesis testing one (1) at 99.9% (C.I.)



Dependent Variable	(I) LSC Techniques	(J) LSC Techniques	Mean Difference (I-J)	Std. Error	Sig. ^b	99.9% Confidence Interval for Difference ^b	
						Lower Bound	Upper Bound
						Geoidal Undulation	SLSC
	NLSLC	SLSC	0.020	0.036	0.567	-0.097	0.137
Processing Time (Seconds)	SLSC	NLSLC	-30.459*	0.000	0.000	-30.459	-30.459
	NLSLC	SLSC	30.459*	0.000	0.000	30.459	30.459

Based on estimated marginal means. *. The average difference is significant at the .001 level. b. Adjustment for multiple comparisons: Least Significant Difference (equivalent to no adjustment).

Table 5 provides paired sample correlations for hypothesis testing, indicating weak negative correlations between the best-fit geoidal undulation and existing models (GRAV and GPS/LEVEL).

Table 5: Output of Paired Samples Correlations for Hypothesis testing two (2)

Paired Samples Correlations				
Geoidal Undulation		N	Correlation	Sig.
Pair 1	Best-fit & Existing (GRAV)	3186	-0.270	0.000
Pair 2	Best-fit & Existing (GPS/LEVEL)	3186	-0.303	0.000
Pair 3	Orth & Height (Computed Vs Existing)	3186	1.000	0.000

Table 6 presents the paired samples test for hypothesis testing at a 95% confidence level, showing significant differences between best-fit and existing geoidal models (GRAV and GPS/LEVEL), as well as between computed and existing orthometric heights, with all tests yielding highly significant p-values (0.000)

Table 6: Paired Samples Test for Hypothesis testing two (2) at 95%

Paired Samples Test									
		Paired Differences					t	df	Sig. (2-tailed)
		Mean	Std. Dev.	Std. Error Mean	95% Confidence Interval for the Difference				
					Lower	Upper			
Pair 1	Best-fit & Existing (GRAV)	0.9882	1.4670	0.0259	0.9372	1.0392	38.022	3185	0.000
Pair 2	Best-fit & Existing (GPS/LEVEL)	0.8949	1.5187	0.0269	0.8421	0.9476	33.261	3185	0.000



Pair 3	Orth & Height (Computed Vs Existing)	-14.2833	0.6252	0.0110	-14.3051	-14.2616	-1289.455	3185	0.000
---------------	-----------------------------------------	----------	--------	--------	----------	----------	-----------	------	-------

Table 7 presents the paired samples test for hypothesis testing at a 99.9% confidence level, confirming significant differences between the best-fit and existing (GPS/LEVEL) geoidal undulation and between computed and existing orthometric heights, with highly significant p-values (0.000)

Table 7: Paired Samples Test for Hypothesis testing two (2) at 99.9%

Paired Samples Test									
		Paired Differences					t	df	Sig. (2-tailed)
		Mean	Std. Dev.	Std. Error Mean	99.9% Confidence Interval for the Difference				
					Lower	Upper			
Pair 2	Best-fit & Existing (GPS/LEVEL)	0.8949	1.5187	0.0269	0.8063	0.9835	33.261	3185	0.000
Pair 3	Orth & Height (Computed Vs Existing)	-14.2833	0.6252	0.0111	-14.3198	-14.2469	-1289.455	3185	0.000

4.2 DISCUSSION

4.2.1 Geoidal Undulation based on SLSC and NSLSC and Processing Time

From Tables 2a and 2b, it can be observed that the geoidal undulation within the study area using the Stationary Least Squares Collocation (SLSC) technique utilized a mean of 14.273m (SE = 0.025m) with a 95% confidence interval of [14.224m, 14.323m], while the Non-Stationary Least Squares Collocation (NSLSC) technique produced a slightly higher mean of 14.294m (SE = 0.025m) with a 95% confidence interval of [14.244m, 14.343m]. The processing time for the SLSC was significantly shorter at 8.210 seconds (SE = 0.000), compared to the NSLSC, which required 38.669 seconds (SE = 0.000). The 99.9% confidence intervals for geoidal undulation were [14.190m, 14.356m] for the SLSC and [14.211m, 14.376m] for the NSLSC. All estimates were calculated with the covariate of computed orthometric height evaluated at 320.11 m.

Meanwhile, from Figure 6, the comparison of the Estimated Marginal Means of geoidal undulation for the Akure study area using two Least Squares Collocation (LSC) techniques: SLSC and NSLSC is revealed. The NSLSC method produces a slightly higher geoidal undulation value (14.2936m) compared to the SLSC method (14.2733m), indicating a marginal increase. This difference implies that the NSLSC technique might provide a marginally better fit or estimation of geoidal undulation for the study area under the given model conditions. Such



variations suggest that the computational approach and underlying assumptions in NSLSC may capture additional nuances in geoidal undulation estimation compared to SLSC.

In addition, Figure 7 still gave graphical illustration of Estimated Marginal Means of Processing Time (Seconds) for two different LSC techniques in the Akure Study Area: SLSC and NSLSC. The SLSC technique has an estimated mean processing time of approximately 8.21 seconds, while the NSLSC technique has a mean processing time of about 38.67 seconds. This shows that the NSLSC technique takes significantly longer—about 30.46 seconds more—than the SLSC technique. The difference in processing times suggests that SLSC is a faster method, potentially more efficient for handling large datasets or for applications requiring quick results. In contrast, NSLSC may be better suited for situations where accuracy is prioritized over speed, as the longer processing time may be attributed to more complex calculations or additional data handling. The covariate, Computed Orthometric Height, was held constant at 320.11m in both cases, indicating that the processing time differences are likely due to the techniques themselves and not variations in the covariate. In summary, while NSLSC provides more precise results, its significantly higher processing time may limit its practical use in situations demanding faster computations.

4.2.2 Geoidal Undulation based on Covariance model and Processing Time

Figure 8 compares the Estimated Marginal Means of geoidal undulation for the Akure study area across three covariance models: Gaussian, Exponential, and Matérn. The Gaussian and Exponential models show very similar results, with values of 14.2733m and 14.2732m, respectively, while the Matérn model yields a higher value of 14.3037m. This indicates that the Matérn model may better account for spatial variability or provide a more refined estimation of geoidal undulation within Akure. These differences suggest the importance of selecting an appropriate covariance model to improve the accuracy of geodetic computations.

While Figure 9 displays the Estimated Marginal Means of Processing Time (Seconds) for the three different covariance models used in the area: The Gaussian model shows an estimated processing time of approximately 16.30 seconds, the Exponential model has a processing time of about 13.65 seconds, and the Matern model has the highest processing time at 40.36 seconds. This indicates that the Matern covariance model requires significantly more time compared to the Gaussian and Exponential models, with a difference of 23.06 seconds compared to Exponential and 24.06 seconds compared to Gaussian. The difference in processing times between these models suggests that the Exponential and Gaussian models are more computationally efficient, while the Matern model could be more complex, requiring more time to process. This may reflect the intricacy of the model's calculations, where Matern provides a more detailed fit but at the cost of increased processing time.

4.2.3 Geoidal Undulations Based on the Type(s) of GGM Models Used

Figures 10 to 12 show that EGM2008-GGM has a mean of 15.228722326m. SGG-UM-2-GGM had a mean of 13.652996248m. Meanwhile, XGM2019e-GGM showed a mean of 13.660302596m. The aggregate mean is 14.180673723m. The mean value differences demonstrate that the GGM model used has a significant impact on the NSLSC technique's geoid undulation predictions, demanding careful model selection for reliable geoid modelling. This agrees with [38] and [35] "that EGM2008 provides better results and has an agreement with the



GPS/Levelling data over the study area, and also [39] assertion "that EGM2008 indicates high potential in geoid modelling over Kenya" which has similar regional formations like Nigeria.

4.2.4 Geoidal Undulations Based on the Type(s) of DEM - Models Used

According to Figure 13 to 15, the mean of ALOS-PAL-DEM is 15.023519712m, and the ASTER-DEM method produced a mean of 15.236686247m. Meanwhile, TANDEM-DEM recorded a mean of 12.281815211m. The results showed that the aggregate mean is 14.180673723m. The substantial differences in average values across the DEM models emphasize the necessity of selecting the appropriate DEM to accurately predict geoid undulation using the NSLSC technique.

4.2.5 Pairwise Comparison of SLSC and NSLSC Techniques

Tables 3 and 4 reveal the pairwise comparisons for geoidal undulation in the Akure study area; and indicate that the difference between the Stationary Least Squares Collocation (SLSC) and Non-Stationary Least Squares Collocation (NSLSC) techniques is not statistically significant, with a mean difference of -0.020 (SE = 0.036, $p = 0.567$) and a 95% confidence interval of [-0.090, 0.049]. This result remains consistent under a 99.9% confidence interval, which spans [-0.137, 0.097]. However, in terms of processing time, there is a highly significant difference between the two techniques. The SLSC technique was 30.459 seconds faster than the NSLSC (SE = 0.000, $p < 0.001$), with a confidence interval of [-30.459, -30.459] for both the 95% and 99.9% levels. These results are based on estimated marginal means and include adjustments for multiple comparisons using the Least Significant Difference method.

4.2.6 Statistical Analysis of Geoidal Undulation and Orthometric Height Correlations

From Table 5, the correlation analysis reveals varying relationships between the datasets. The correlation coefficient for the best-fit and existing gravimetric geoid undulation is -0.270, indicating a weak negative relationship, with a statistically significant p -value of 0.000. Similarly, the best-fit and existing GPS/Level geoid undulations show a weak negative correlation of -0.303, also statistically significant with a p -value of 0.000. In contrast, the computed and existing orthometric heights exhibit a perfect positive correlation of 1.000, with a p -value of 0.000, confirming a strong agreement between the two datasets.

4.2.7 Paired Samples Analysis of Geoidal Undulation and Orthometric Heights

Tables 6 and 7 present the paired sample analysis for the Akure study area, highlighting significant differences between best-fit and Existing Undulation (GRAV) model, as well as between Computed Orthometric Height (best-fit) and Existing Orthometric Height. For Pair 1, the mean difference was 0.988m (SD = 1.467m), with a 95% confidence interval of [0.937m, 1.039m] and a 99.9% confidence interval of [0.903m, 1.074m]. The correlation was negative (-0.270m), and the paired differences were statistically significant ($t = 38.022$, $p < 0.001$). For Pair 2, the average difference was 0.895m (SD = 1.519m), with a 95% confidence interval of [0.842m, 0.948m] and a 99.9% confidence interval of [0.806m, 0.984m]. The correlation was also negative (-0.303m), with significant paired differences ($t = 33.261$, $p < 0.001$). For Pair 3, which compares Computed and Existing Orthometric Heights, the average difference was -14.283m (SD = 0.625m), with a 95% confidence interval of [-14.305m, -14.262m] and a 99.9% confidence interval of [-14.320m, -14.247m]. The correlation was



exceptionally high ($r = 1.000$), and the difference was extremely significant ($t = -1289.455$, $p = < 0.001$). In the long term, the results confirm statistically significant disparities across all pairs, indicating meaningful differences between the Computed Orthometric Height and Existing Orthometric Height within the study area.

5.0 CONCLUSION

The TUIDOTA computational tool is developed for global users to implement Stationary and Nonstationary Least Square Collocation (SLSC & NSLSC) technique integrated with Molodensky's method. It offers flexible parameters to accommodate diverse user needs. A validation study was conducted in a mountainous region in South-Western Nigeria, using GNSS/levelling data for ground truthing. Results demonstrated the tool's effectiveness in determining local gravimetric geoid model with absolute accuracy and computational efficiency, making it a practical tool for geoid modelling. High-quality terrestrial gravity, geopotential, and digital elevation models were utilized. The methodology applied three different covariance models, integrated with Molodensky's model via the Remove-Compute-Restore (R-C-R) approach, to estimate geoidal undulations. A comparative analysis of geoidal undulation estimates, processing times, and covariance models was conducted. Findings revealed that in Akure, the SLSC produced a mean geoidal undulation of 14.273m, while the NSLSC yielded a slightly more significant value of 14.294m, suggesting a marginal accuracy improvement with the NSLSC. However, the SLSC was significantly faster (8.210s) compared to the NSLSC (38.669s), making it preferable for time-sensitive applications. Among covariance models, the Matérn model provided the most significant most significant geoidal undulation (14.3037m) but required the longest processing time (40.36s), indicating a trade-off between accuracy and computational efficiency. The Gaussian and Exponential models balance precision and efficiency, making them suitable for practical applications. Overall, TUIDOTA addresses the lack of user-friendly computational tool for Least Square Collocation with Molodensky's method. It successfully balances accuracy and computational efficiency, making it suitable for first time users to compute gravimetric geoid models without extensive training. The study highlights the strengths and trade-offs of the different covariance models and LSC based techniques used in this study for local geoid determination. Future developments should focus on enhancing automation, integrating real-time GNSS corrections, and expanding usability for complex urban terrains. suggested, such as testing TUIDOTA in different terrains or integrating machine learning for improved accuracy.

REFERENCES

- [1]. Abbak, A. R., Ellmann, A., & Ustun, A. (2022). A practical software package for computing the gravimetric geoid by the least squares modification of Hotine's formula. *Earth Science Informatics*, 15(1), 713–724.
- [2]. Abbak, R. A., & Ustun, A. (2015). A software package for computing a regional gravimetric geoid model utilizing the KTH method. *Earth Science Informatics*, 8(1), 255–265.



www.journals.unizik.edu.ng/jsis

- [3]. Abbak, R. A., Goyal, R., & Ustun, A. (2024). A user-friendly software package for modeling gravimetric geoid by the classical Stokes-Helmert method. *Earth Science Informatics*, 17, 3811–3824. <https://doi.org/10.1007/s12145-024-01328-0>
- [4]. Abd-Elmotaal, H. A. (1998). An efficient technique for the computation of the gravimetric quantities from geopotential earth models. *Geodesy on the Move*, 182-187. https://doi.org/10.1007/978-3-642-72245-5_25
- [5]. Dagogo, M. J. F., Fajemirokun, F. A., & Ezeigbo, C. U. (2014). *Fundamentals of Geodesy* (Textbook). Concept Publications Limited, Lagos, Nigeria.
- [6]. Darbeheshti, N., & Featherstone, W. E. (2009). Non-stationary covariance function modeling in 2D least-squares collocation. *Journal of Geodesy*, 83(6), 495-508. <https://doi.org/10.1007/s00190-008-0267-0>
- [7]. Darbeheshti, N., & Featherstone, W. E. (2010). Tuning a gravimetric quasi-geoid to GPS-levelling by non-stationary least-squares collocation. *Journal of Geodesy*, 84(7), 419-431. <https://doi.org/10.1007/s00190-010-0377-3>
- [8]. Drewes, H., & Heidbach, O. (2005). Deformation of the South American crust estimated from finite element and collocation methods. *International Association of Geodesy Symposia*, 544-549. https://doi.org/10.1007/3-540-27432-4_92
- [9]. Ezeigbo, C. U. (1988). *Least Squares Collocation Method for Geoid and Datum Determination for Nigeria* (Ph.D. Thesis). Department of Surveying, University of Lagos, Nigeria.
- [10]. Feyza, S., Serdar, E., Artu, E., & Bihter, E. (2021). Geoid modeling by the least squares modification of Hotine's and Stokes' formulae using non-gridded gravity data. *Computers & Geosciences*, 156, 104909. <https://doi.org/10.1016/j.cageo.2021.104909>
- [11]. Featherstone, W. (2003). Software for computing five existing types of deterministically modified integration kernels for gravimetric geoid determination. *Computers & Geosciences*, 29(2), 183–193.
- [12]. Forsberg, R. (1987). A new covariance model for inertial gravimetry and gradiometry. *Journal of Geophysical Research: Solid Earth*, 92(B2), 1305-1310. <https://doi.org/10.1029/jb092ib02p01305>
- [13]. Guimarães, G. D., Blitzkow, D., Barzaghi, R., & Matos, A. C. (2014). The computation of the geoid model in the state of São Paulo using two methodologies and GOCE models. *Boletim de Ciências Geodésicas*, 20(1), 183-203. <https://doi.org/10.1590/s1982-21702014000100012>
- [14]. Heiskanen, W., & Moritz, H. (1967). *Physical Geodesy*. Freeman, San Francisco.
- [15]. ICGEM. Retrieved January 24, 2024, from <http://icgem.gfz-potsdam.de/home>



www.journals.unizik.edu.ng/jsis

- [16]. Idowu, T. (2006). Prediction of gravity anomalies for geophysical exploration. *FUTY Journal of the Environment*, 1(1). <https://doi.org/10.4314/fje.v1i1.50776>
- [17]. Idowu, T. O., Nwilo, P. C., Fajemirokun, F. A., & Ezeigbo, C. U. (2008). Determination of optimum residual gravity anomalies for mineral exploration: A least squares collocation approach. *Survey Review*, 40(309), 294-303. <https://doi.org/10.1179/003962608x325367>
- [18]. Jekeli, C., Lee, J., & Kwon, J. H. (2006). Modeling errors in the upward continuation of INS gravity compensation. *Journal of Geodesy*, 81(5), 297-309. <https://doi.org/10.1007/s00190-006-0108-y>
- [19]. Knudsen, P. (2005). Patching local empirical covariance functions—A problem in altimeter data processing. *International Association of Geodesy Symposia*, 483-487. https://doi.org/10.1007/3-540-27432-4_82
- [20]. Knudsen, P. (1987). Estimation and modeling of the local empirical covariance function using gravity and satellite altimeter data. *Bulletin Géodésique*, 61(2), 145-160. <https://doi.org/10.1007/bf02521264>
- [21]. Krarup, T. (1969). *Contributions to the Mathematical Foundations of Physical Geodesy*.
- [22]. Krarup, T. (1970). Method of least squares collocation. *Studia Geophysica et Geodaetica*, 14(2), 107-109. <https://doi.org/10.1007/bf02585604>
- [23]. Łyszkowicz, A. (2010). Quasigeoid for the area of Poland computed by least squares collocation. *Technical Sciences*, 13(1), 147-164. <https://doi.org/10.2478/v10022-010-0014-7>
- [24]. Marchenko, A. N., Barthelmes, F., Meyer, U., & Schwintzer, P. (2002). Efficient regional geoid computations from airborne and surface gravimetry data: A case study. *International Association of Geodesy Symposia*, 223-228. https://doi.org/10.1007/978-3-662-04709-5_37
- [25]. Mehdi, G., Ismael, F., & Pavel, N. (2019). Application of the one-step integration method for determination of the regional gravimetric geoid. *Journal of Geodesy*, 93(9), 1631-1644. <https://doi.org/10.1007/S00190-019-01272-8>
- [26]. Meissi, P., (1971). "A Study of Covariance Functions Related to the Earth's Disturbing Potential," Department of Geodetic Science, Ohio State University, report no.151.
- [27]. Moritz, H. (1980). *Advanced Physical Geodesy*. Abacus, Tunbridge Wells.
- [28]. Odumosu, J. O., Nnam, V. C., & Nwadiolor, I. J. (2021). An assessment of spatial methods for merging terrestrial with GGM-derived gravity anomaly data. *Journal of African Earth Sciences*, 179, 104202. <https://doi.org/10.1016/j.jafrearsci.2021.104202>



- [29]. Ono, M. N., Agaje, A. B., & Onwuzuligbo, C. U. (2017). Gravimetric geoid determination of Okenya Town, Idah Kogi State, Nigeria. *Nigerian Journal of Geodesy*, 1(1), 113-136.
- [30]. Ramouz, S., Afrasteh, Y., Reguzzoni, M., Safari, A., & Saadat, A. (2019). IRG2018: A regional geoid model for Iran using least squares collocation. *Studia Geophysica et Geodaetica*, 63(2), 191-214. <https://doi.org/10.1007/s11200-018-0116-4>
- [31]. Risser, M. D., & Calder, C. A. (2017). Local likelihood estimation for covariance functions with spatially-varying parameters: The convoSPAT package for R. *Journal of Statistical Software*, 81(14), 1–32. <https://doi.org/10.18637/jss.v081.i14>
- [32]. Risser, M. D., & Calder, C. A. (2015). Regression-based covariance functions for nonstationary spatial modeling. *Environmetrics*, 26(4), 284-297. <https://doi.org/10.1002/env.2336>
- [33]. Saadon, A., El-Ashquer, M., Elsaka, B., & El-Fiky, G. (2021). Determination of local gravimetric geoid model over Egypt using LSC and FFT estimation techniques based on different satellite- and ground-based datasets. *Survey Review*, 54(384), 263-273. <https://doi.org/10.1080/00396265.2021.1932148>
- [34]. Sansò, F., & Sideris, M. G. (2013). *Geoid Determination: Theory and Methods*. Springer-Verlag, Berlin Heidelberg. <https://doi.org/10.1007/978-3-540-74700-0>
- [35]. Tata, H., & Ono, M. N. (2018). A gravimetric approach for the determination of orthometric heights in Akure Environs, Ondo State, Nigeria. *Journal of Environment and Earth Sciences*, 8(8), 2224-3216.
- [36]. Tata, H., Ono, M. N., & Idowu, T. O. (2019). Development of a computational tool for the determination of the local geoid using gravimetric and GPS/leveling approaches. *Nigerian Journal of Geodesy*, 3(1), ISSN 2651-6098.
- [37]. Timilsina, S., Willberg, M., & Rol, R. (2021). Regional geoid for Nepal using least-squares collocation. *Terrestrial, Atmospheric and Oceanic Sciences*, 32(5.2). <https://doi.org/10.3319/tao.2021.08.23.02>.
- [38]. Tscherning, C. C. (1994). Geoid determination by least-squares collocation using GRAVSOFT. *Lecture Notes for the International School for the Determination and Use of the Geoid*, DIIAR - Politecnico di Milano, Milano.
- [39]. Uuemaa, E., Ahi, S., Montibeller, B., Muru, M., & Kmoch, A. (2020). Vertical accuracy of directly available global digital elevation models (ASTER, AW3D30, MERIT, TanDEM-X, SRTM, and NASA DEM). *Remote Sensing*, 12(21), 3482.
- [40]. Vaniček, P., & Featherstone, W. (1998). Performance of three types of Stokes's kernel in the combined solution for the geoid. *Journal of Geodesy*, 72(12), 684–697.



www.journals.unizik.edu.ng/jsis

- [41]. Yildiz, H., Forsberg, R., Ågren, J., Tscherning, C., & Sjöberg, L. (2012). Comparison of remove-compute-restore and least squares modification of Stokes' formula techniques for quasi-geoid determination over the Auvergne test area. *Journal of Geodetic Science*, 2(1), 53–64.
- [42]. Zhu, L., & Jekeli, C. (2008). Gravity gradient modeling using gravity and DEM. *Journal of Geodesy*, 83(6), 557-567. <https://doi.org/10.1007/s00190-008-0273-2>